

**MECHANISTIC DESIGN DATA FROM
ODOT INSTRUMENTED PAVEMENT
SITES- PHASE II REPORT**

Phase II Final

SPR 763

MECHANISTIC DESIGN DATA FROM ODOT INSTRUMENTED PAVEMENT SITES- PHASE II REPORT

Phase II Final

SPR 763

by
Dr. David H. Timm, P.E.
Michael C. Vrtis
National Center for Asphalt Technology (NCAT)
Auburn University
277 Technology Parkway
Auburn, AL 36830

for

Oregon Department of Transportation
Research Section
555 13th Street NE, Suite 1
Salem OR 97301

and

Federal Highway Administration
400 Seventh Street, SW
Washington, DC 20590-0003

March 2017

| | | | |
|--|---|--|-----------|
| 1. Report No. FHWA | 2. Government Accession No. | 3. Recipient's Catalog No. | |
| 4. Title and Subtitle MECHANISTIC DESIGN DATA FROM ODOT INSTRUMENTED PAVEMENT SITES- PHASE II REPORT | | 5. Report Date February 2017 | |
| | | 6. Performing Organization Code | |
| 7. Author(s) Dr. David H. Timm and Michael C. Vrtis | | 8. Performing Organization Report No. | |
| 9. Performing Organization Name and Address National Center for Asphalt Technology (NCAT) Auburn University 277 Technology Parkway Auburn, AL 36830 | | 10. Work Unit No. (TRAIS) | |
| | | 11. Contract or Grant No. SPR 763 – Phase II | |
| 12. Sponsoring Agency Name and Address Oregon Dept. of Transportation Research Section and Federal Highway Admin. 555 13 th Street NE, Suite 1 400 Seventh Street, SW Salem, OR 97301 Washington, DC 20590-0003 | | 13. Type of Report and Period Covered Phase II Final Report | |
| | | 14. Sponsoring Agency Code | |
| 15. Supplementary Notes | | | |
| 16. Abstract This investigation examined data obtained from three previously-instrumented pavement test sites in Oregon. Data processing algorithms and templates were developed for each test site that facilitated full processing of all the data to build databases representing each site. Investigation of site data found that most of the collected data could be successfully processed and observed trends in the data were as expected (e.g., seasonal changes affected pavement response). The location that compared rubblized base to aggregate base clearly demonstrated the effect of the rubblized base through a 50% reduction in strain at the bottom of the asphalt layer. Further investigations of the data may be warranted and user's guides provided in this report will enable those investigations to proceed by ODOT staff. | | | |
| 17. Key Words Pavement, instrumentation | | 18. Distribution Statement Copies available from NTIS, and online at http://www.oregon.gov/ODOT/TD/TP_RES/ | |
| 19. Security Classification (of this report) Unclassified | 20. Security Classification (of this page) Unclassified | 21. No. of Pages 344 | 22. Price |

SI* (MODERN METRIC) CONVERSION FACTORS

| APPROXIMATE CONVERSIONS TO SI UNITS | | | | APPROXIMATE CONVERSIONS FROM SI UNITS | | | | |
|--|----------------------|-------------|---------------------|---------------------------------------|---------------------|-------------|----------------------|-----------------|
| Symbol | When You Know | Multiply By | To Find | Symbol | When You Know | Multiply By | To Find | Symbol |
| <u>LENGTH</u> | | | | <u>LENGTH</u> | | | | |
| in | inches | 25.4 | millimeters | mm | millimeters | 0.039 | inches | in |
| ft | feet | 0.305 | meters | m | meters | 3.28 | feet | ft |
| yd | yards | 0.914 | meters | m | meters | 1.09 | yards | yd |
| mi | miles | 1.61 | kilometers | km | kilometers | 0.621 | miles | mi |
| <u>AREA</u> | | | | <u>AREA</u> | | | | |
| in ² | square inches | 645.2 | millimeters squared | mm ² | millimeters squared | 0.0016 | square inches | in ² |
| ft ² | square feet | 0.093 | meters squared | m ² | meters squared | 10.764 | square feet | ft ² |
| yd ² | square yards | 0.836 | meters squared | m ² | meters squared | 1.196 | square yards | yd ² |
| ac | acres | 0.405 | hectares | ha | hectares | 2.47 | acres | ac |
| mi ² | square miles | 2.59 | kilometers squared | km ² | kilometers squared | 0.386 | square miles | mi ² |
| <u>VOLUME</u> | | | | <u>VOLUME</u> | | | | |
| fl oz | fluid ounces | 29.57 | milliliters | ml | milliliters | 0.034 | fluid ounces | fl oz |
| gal | gallons | 3.785 | liters | L | liters | 0.264 | gallons | gal |
| ft ³ | cubic feet | 0.028 | meters cubed | m ³ | meters cubed | 35.315 | cubic feet | ft ³ |
| yd ³ | cubic yards | 0.765 | meters cubed | m ³ | meters cubed | 1.308 | cubic yards | yd ³ |
| NOTE: Volumes greater than 1000 L shall be shown in m ³ . | | | | | | | | |
| <u>MASS</u> | | | | <u>MASS</u> | | | | |
| oz | ounces | 28.35 | grams | g | grams | 0.035 | ounces | oz |
| lb | pounds | 0.454 | kilograms | kg | kilograms | 2.205 | pounds | lb |
| T | short tons (2000 lb) | 0.907 | megagrams | Mg | megagrams | 1.102 | short tons (2000 lb) | T |
| <u>TEMPERATURE (exact)</u> | | | | <u>TEMPERATURE (exact)</u> | | | | |
| °F | Fahrenheit | (F-32)/1.8 | Celsius | °C | Celsius | 1.8C+32 | Fahrenheit | °F |

*SI is the symbol for the International System of Measurement

ACKNOWLEDGEMENTS

The authors wish to thank the Oregon Department of Transportation for their support and cooperation with this project.

DISCLAIMER

This document is disseminated under the sponsorship of the Oregon Department of Transportation and the United States Department of Transportation in the interest of information exchange. The State of Oregon and the United States Government assume no liability of its contents or use thereof.

The contents of this report reflect the view of the authors who are solely responsible for the facts and accuracy of the material presented. The contents do not necessarily reflect the official views of the Oregon Department of Transportation or the United States Department of Transportation.

The State of Oregon and the United States Government do not endorse products of manufacturers. Trademarks or manufacturers' names appear herein only because they are considered essential to the object of this document.

This report does not constitute a standard, specification, or regulation.

TABLE OF CONTENTS

| | | |
|------------|---|-----------|
| 1.0 | INTRODUCTION..... | 1 |
| 2.0 | DATA PROCESSING AND DATABASE DEVELOPMENT | 3 |
| 3.0 | DATA ANALYSIS AND DISCUSSION..... | 6 |
| 3.1 | MEDFORD | 6 |
| 3.1.1 | Site Description and Scope of Data | 6 |
| 3.1.2 | Results and Discussion | 8 |
| 3.2 | REDMOND | 13 |
| 3.2.1 | Site Description and Scope of Data | 13 |
| 3.2.2 | Results and Discussion | 14 |
| 3.3 | DEVER-CONNER | 18 |
| 3.3.1 | Site Description and Scope of Data | 18 |
| 3.3.2 | Results and Discussion | 20 |
| 3.4 | COMPARISON BETWEEN TEST SITES | 25 |
| 4.0 | TECHNOLOGY TRANSFER..... | 27 |
| 5.0 | SUMMARY | 28 |
| 6.0 | REFERENCES..... | 29 |

LIST OF FIGURES

| | |
|--|----|
| Figure 1.1: ODOT Instrumented Pavement Test Sites (<i>Google Earth 2015</i>) | 2 |
| Figure 2.1.1: Medford Processing Template..... | 4 |
| Figure 2.2: Redmond Processing Template..... | 5 |
| Figure 2.3: Dever-Conner Processing Template..... | 5 |
| Figure 3.1: Medford and Redmond Instrumentation Layout (<i>Timm and Vrtis 2015</i>)..... | 7 |
| Figure 3.2: Medford Distribution of Axles per Vehicle..... | 7 |
| Figure 3.3: Medford Axle Type Distribution..... | 8 |
| Figure 3.4: Medford Strain Percentiles by Axle Type – All Vehicles..... | 9 |
| Figure 3.5: Medford Strain Percentiles by Axle Type-Excluding Two Axle Vehicles..... | 10 |
| Figure 3.6: Medford Longitudinal and Transverse Strain Comparison..... | 10 |
| Figure 3.7: Theoretical Strain Response from Tandem Axle..... | 11 |
| Figure 3.8: Theoretical Strain Response from Tridem Axle..... | 11 |
| Figure 3.9: Theoretical Strain Response from Quad Axle..... | 12 |
| Figure 3.10: Medford Longitudinal Strain and Speed including all Vehicles..... | 12 |
| Figure 3.11: Medford Longitudinal Strain and Speed Excluding Two Axle Vehicles..... | 13 |
| Figure 3.12: Redmond Distribution of Axles per Vehicle..... | 14 |
| Figure 3.13: Redmond Axle Type Distribution..... | 14 |
| Figure 3.14: Redmond Strain Percentiles by Axle Type..... | 15 |
| Figure 3.15: Redmond Strain Percentiles by Axle Type Excluding Two Axle Vehicles..... | 16 |
| Figure 3.16: Redmond Longitudinal and Transverse Strain Comparison..... | 16 |
| Figure 3.17: Redmond Longitudinal Strain and Speed including all Vehicles..... | 17 |
| Figure 3.18: Redmond Longitudinal Strain and Speed Excluding Two Axle Vehicles..... | 17 |
| Figure 3.19: Redmond Longitudinal Strain by Date..... | 18 |
| Figure 3.20: Dever-Conner Instrumentation Layout..... | 19 |

| | |
|---|----|
| Figure 3.21: Dever-Conner Distribution of Axles per Vehicle..... | 19 |
| Figure 3.22: Dever-Conner Axle Type Distribution..... | 20 |
| Figure 3.23: Dever-Conner Strain Percentiles by Axle Type over Aggregate Base..... | 21 |
| Figure 3.24: Dever-Conner Strain Percentiles by Axle Type over Rubblized Base..... | 22 |
| Figure 3.25: Dever-Conner Longitudinal and Transverse Strain Comparison. | 22 |
| Figure 3.26: Dever-Conner Longitudinal Strain and Speed including all Vehicles..... | 23 |
| Figure 3.27: Dever-Conner 90 th Percentile Strain from Five Axle Vehicles over Time..... | 23 |
| Figure 3.28: Dever-Conner Strain Comparison from Aggregate to Rubblized Base..... | 24 |
| Figure 3.29: Comparison of Average Strain Recorded in November 2009 | 25 |
| Figure 3.30: Pavement Cross Sections. | 26 |

1.0 INTRODUCTION

As documented previously (*Timm and Vrtis 2015*) the Oregon DOT (ODOT) instrumented three pavement sites between 2004 and 2008 to support efforts toward implementing mechanistic-empirical (M-E) pavement design. These three sites are known as the Dever-Conner, Medford and Redmond test sites, respectively. The Dever-Conner and Medford sites are both located on I-5 while the Redmond site is on US 97 as depicted in Figure 1.1.

The purpose of the test sites was to support stepwise validation of the new M-E design approach under development by AASHTO. Specifically, ODOT was interested in measuring tensile strain at the bottom of asphalt concrete (AC) layers as a predictor for bottom-up fatigue cracking (*Scholz 2010*). These measurements were to provide validation of predictions made by computer programs using layered elastic theory.

Though data were collected as part of an earlier research project (*Scholz 2010*), limited data reduction and analysis was conducted and much of the response measurement data were considered to be in raw format. Therefore, there was a need to evaluate the usefulness of the data and assess whether it can be useful for M-E design. There was also a need to develop user-friendly tools for ODOT to continue collecting and analyzing data to support M-E design.

Given these needs, a research contract was awarded to the National Center for Asphalt Technology (NCAT) in 2014 with these main objectives:

1. Process existing data sets and evaluate their usefulness toward implementation of M-E design.
2. Develop user-friendly processing schemes to facilitate future data processing and analysis.

To achieve these objectives, the work was divided into two major phases. Phase I (Preliminary Evaluation) was meant to catalogue and assess the current state of the data, establish rudimentary processing schemes and execute some measured versus predicted strain response comparisons. The results of Phase I were intended to provide ODOT with sufficient information to make a decision whether to continue with Phase II (Full Evaluation). Phase II was to include full data processing and database development followed by technology transfer of the developed products.

In May, 2015, a Phase I project meeting was held at ODOT to present the Phase I report (*Timm and Vrtis 2015*) and discuss continuing with Phase II. At that time, it was decided to begin Phase II of the research which included the following objectives:

1. Document data processing schemes and database development.
2. Characterize in situ pavement responses from each test site.

3. Compare pavement response measurements from each test site.
4. Develop user's guides for the processing templates and accessing the database.

To accomplish these objectives, the data processing scheme developed initially for Phase I was further refined and enhanced to allow for processing of all data from each test site. All the data were then processed and three databases were created to represent each test site. The databases were used to characterize pavement responses from each site and enabled comparisons between them. Finally, user's guides were developed that will enable future data processing and additional investigations using the processing template and database, respectively.



Figure 1.1: ODOT Instrumented Pavement Test Sites (Google Earth 2015).

2.0 DATA PROCESSING AND DATABASE DEVELOPMENT

Signal processing templates were created for each site with the software, DADiSP. Figures 2.1, 2.2, and 2.3 show each test site's template which include a window to paste raw data into, a data preview screen, windows containing each processed signal and a summary output table. The Medford and Redmond templates are identical since the sensor configuration was the same between the two sites. The Dever-Conner template has more processed signal windows since it had more gauges.

Within each template, the preview window allows the data processor to assess whether the file is sufficiently clean to proceed with processing, or subdivide the file into separate vehicle events. The processed signal windows enable a visual check of the data and captured peak values. The summary output table contains the following:

- A user-specified vehicle identification number
- Axle number on each vehicle
- Speed of each axle on each vehicle
- Spacing between axles on each vehicle
- Axle classification (single, tandem, tridem, etc.)
- Baseline and peak values from each sensor for each axle event
- Amplitude readings from each sensor (peak minus baseline)
- Maximum longitudinal strain for each axle event
- Minimum longitudinal strain for each axle event
- Maximum transverse strain for each axle event
- Minimum transverse strain for each axle event

Section 4 and the appendices of this report provides detailed guidance for using the templates and further details regarding the processing algorithms has been previously documented (*Timm and Vrtis, 2015*).

The development of site-specific databases, using data generated from the DADiSP templates, was an important part of Phase II. The databases, created in Microsoft[®] Access allowed for immediate analysis of the data from each site, in addition to long-term archival of the data for future analyses, as needed. Further guidance in using the databases is also provided in Section 3 and the appendices.

The databases contain all of the summary output data generated by the DADiSP templates for all of the files generated at each test site. They are simply named:

- Medford.accdb
- Redmond.accdb
- DeverConner.accdb

A number of queries and pivot charts were also generated within the databases to provide the data presented in the next section of this report. While they are specific to this investigation, they may be adapted for future analyses. Additional queries may also be created within the databases to answer future research questions.

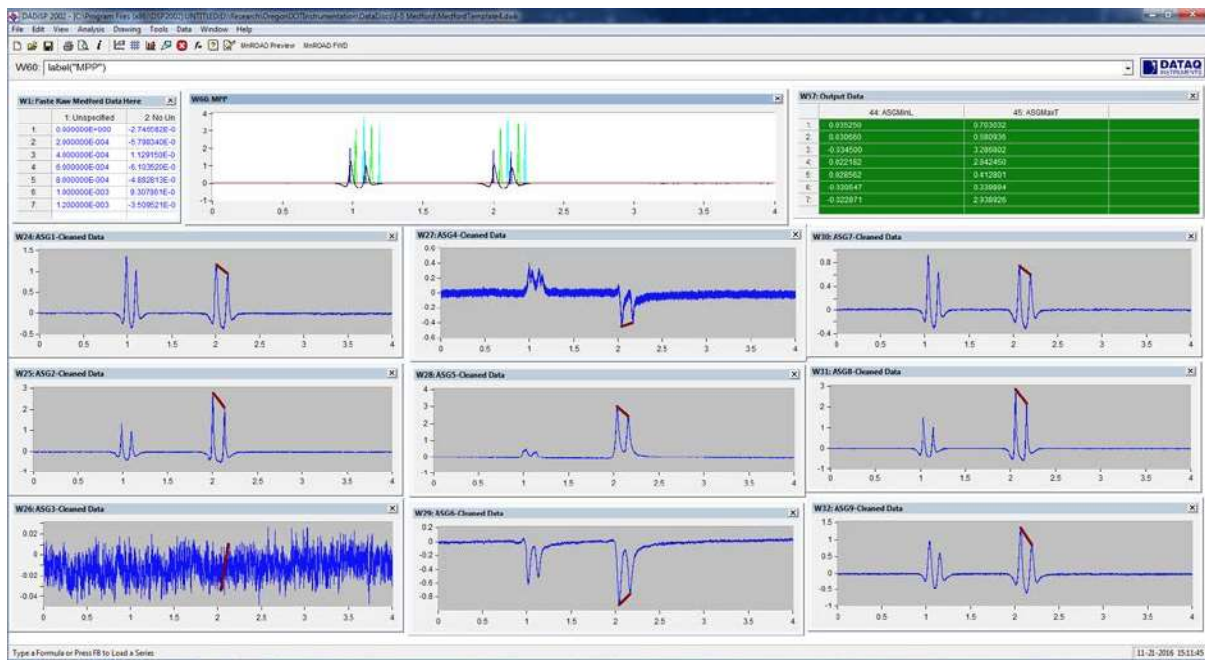


Figure 2.1.1: Medford Processing Template.

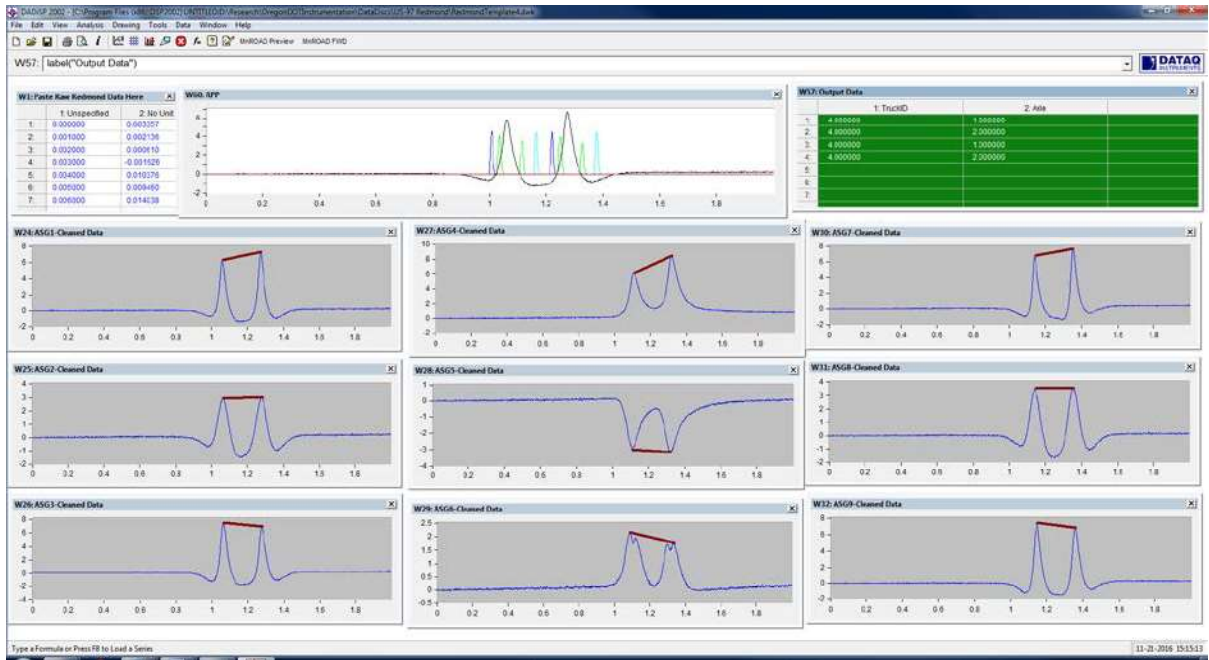


Figure 2.2: Redmond Processing Template.

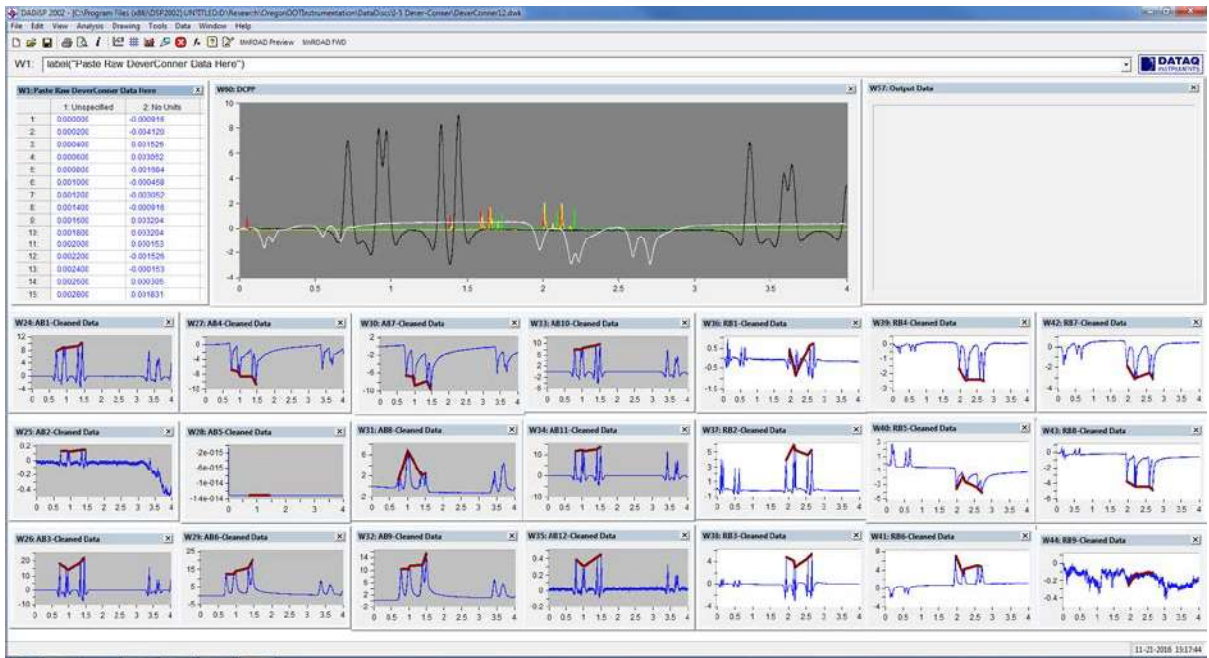


Figure 2.3: Dever-Conner Processing Template.

3.0 DATA ANALYSIS AND DISCUSSION

The following sub-sections will provide a general description of each of the instrumented pavement sites and the available data that was recorded. The results from the processed data are presented, discussed, and compared to expected trends found in the literature and theoretical simulations. Lastly, the results from the three sites are compared and general conclusions drawn.

3.1 MEDFORD

3.1.1 Site Description and Scope of Data

The instrumented pavement section on I-5 in Medford was constructed in August 2009. Axle sensing strips and nine asphalt strain gauges were installed on I-5. As shown in Figure 3.1, six strain gauges were oriented in the longitudinal direction and three gauges oriented in the transverse direction. This instrumentation array was centered on the outside wheelpath of the right lane in the southbound direction of I-5.

Data at this site were only collected on the afternoon of November 24, 2009 from around 3:30 to 5:30 pm. A total of 724 files were collected with some of the files containing multiple vehicle events. Each vehicle event was processed individually creating a total of 972 vehicle events with 2,475 individually axle hits.

Figure 3.2 shows the distribution of axles per vehicle. The vast majority of vehicle events were from two axle vehicles which are likely lightly loaded passenger vehicles. Five axle trucks were the next most common vehicle type but still only comprised 13% of the vehicles captured. The axle type distribution is shown in Figure 3.3. Steer and single axles each comprised 40% of the total and tandem axles comprised 20%. There were only three tridem axles (one set) out of the 2,475 axles recorded which registered as 0% in Figure 3.3.

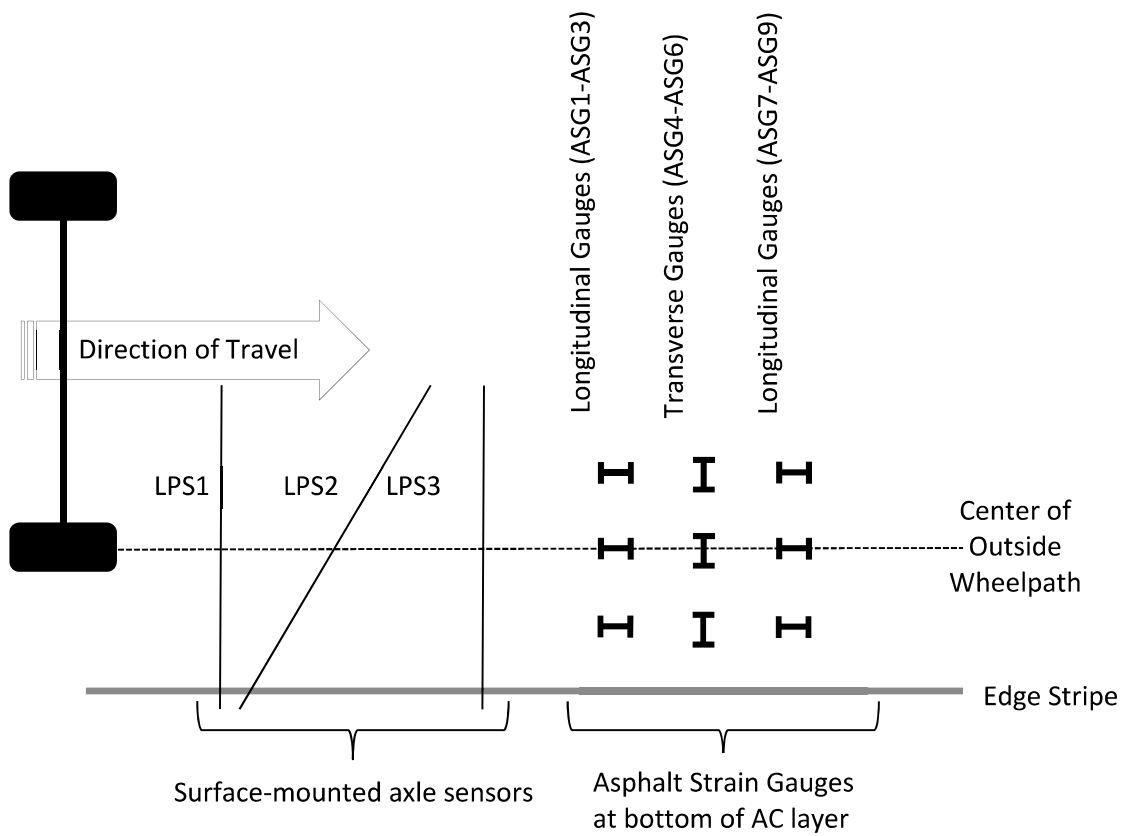


Figure 3.1: Medford and Redmond Instrumentation Layout (*Timm and Vrtis 2015*).

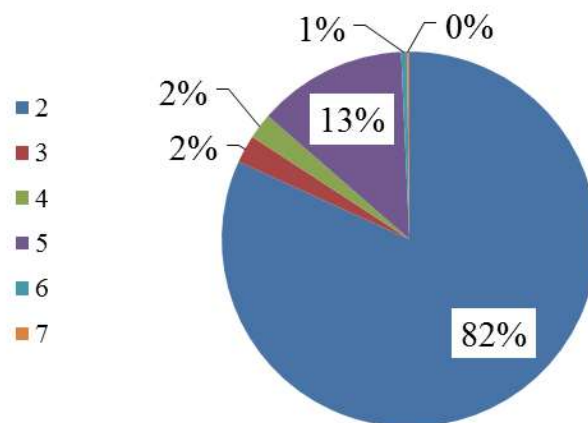


Figure 3.2: Medford Distribution of Axles per Vehicle.

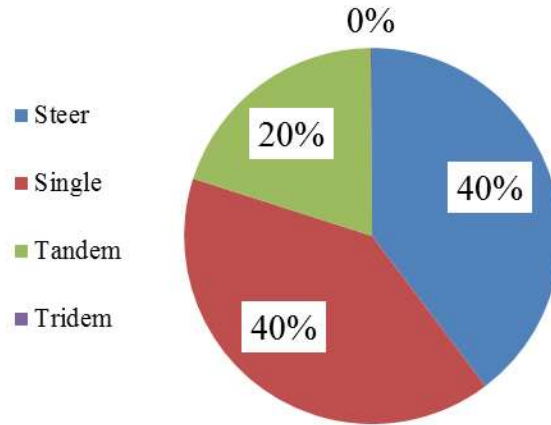


Figure 3.3: Medford Axle Type Distribution.

3.1.2 Results and Discussion

The cumulative percentile of microstrain ($\mu\epsilon$) by axle type is shown for longitudinal and transverse gauges in Figure 3.4. In the legend of Figure 3.4, “1.1” represents a steer axle. “1”, “2”, and “3” represent single, tandem, and tridem axles, respectively. When subsequent axles were within 54 inches of one another they were grouped together and classified as either tandem, tridem, or quad (quad axles were found only in the Redmond and Dever-Conner datasets) based on the number of axles that were closely spaced. “Max L” represents maximum longitudinal strain induced on the gauge array by each axle and “Max T” represents maximum transverse strain from each axle. The 50th percentile longitudinal microstrain for tandem axles (ASG Max L -2) is around 11 $\mu\epsilon$. The highest strain percentiles were induced by the tandem axles which are not influenced by passenger vehicles. After removing the two axle vehicles and recalculating the percentiles, the strain percentiles for the steer and single axles are increased, as shown in Figure 3.5. The lateral offset of each vehicle event was not calculated due to predominantly erratic responses on the diagonal sensing strip which would have significantly reduced the number of quality vehicle events that could be processed.

In both Figures 3.4 and 3.5 the longitudinal strains were greater than the transverse strains for all axle types except the tridem. The ratio of each axle event’s corresponding transverse strain divided by longitudinal strain was calculated and the average for each axle type is shown in Figure 3.6. For all axle types except tridem, there is a lower strain induced in the transverse direction than the longitudinal direction. Previous research at the NCAT Test Track found similar results in which the transverse strain response was found to be 2/3 of the longitudinal strain response (*Timm and Priest 2008*). This relationship is important to verify for pavement design because transverse cracks are likely to develop first, as result of a result of the higher strain measured in the longitudinal direction.

The relationship between transverse and longitudinal strain responses from tridem axles was further investigated using theoretical simulations. The pavement structure was modeled in the

linear-elastic analysis program WESLEA and the strain responses from tandem, tridem, and quad axles were simulated under a load of 20,000 lbs. per axle (5,000 per tire). The same strain profiles were observed at axle loads of 15,000 and 10,000 lbs. but the magnitude of strain was reduced. WESLEA default material properties were used as inputs. The moduli were 500,000, 20,000, and 12,000 psi for the asphalt concrete, granular base, and subgrade, respectively. Poisson's ratio was 0.35 for the asphalt concrete, 0.4 for the granular base, and 0.45 for the subgrade. In the tandem axle simulations in Figure 3.7, the peak longitudinal strain is greater than the peak transverse strain under both axle events. However, in the simulations for the tridem axle, shown in Figure 3.8, the peak transverse strain under the middle axle is greater than the peak longitudinal strain, thus explaining the tridem axle ratio shown in Figure 3.6. The same phenomenon was observed for the middle axles of a quad axle, shown in Figure 3.9. Quad axles were not found in the Medford dataset but were in the Redmond and Dever-Conner datasets, discussed later in this report.

The relationship between speed and longitudinal microstrain is presented in Figure 3.10. It can be seen that there is not a distinguishable trend between speed and strain and there is a large cluster of data points that are under 5 $\mu\epsilon$. After removing the two axle vehicles from the dataset (Figure 3.11), the larger cluster under 5 $\mu\epsilon$ is removed but there is still not a distinguishable trend between speed and strain. It is important to verify that there is not trend between speed and strain because lower speeds and heavy vehicles may induce more distress on the pavement due to the viscoelastic nature of asphalt concrete. The lack of a clearly-defined trend indicates that the range of measured strain values largely resulted from variation in load magnitude and axle placement relative to the gauges.

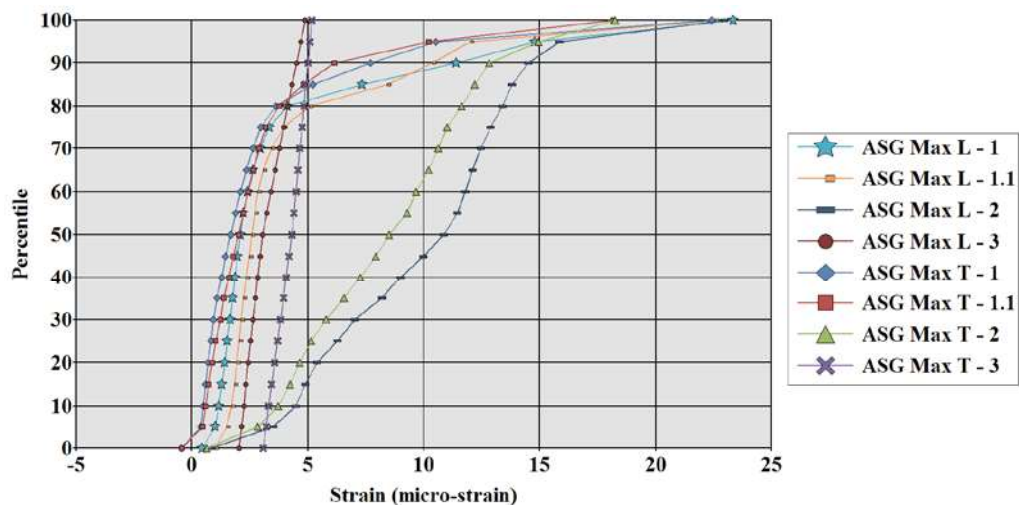


Figure 3.4: Medford Strain Percentiles by Axle Type – All Vehicles.

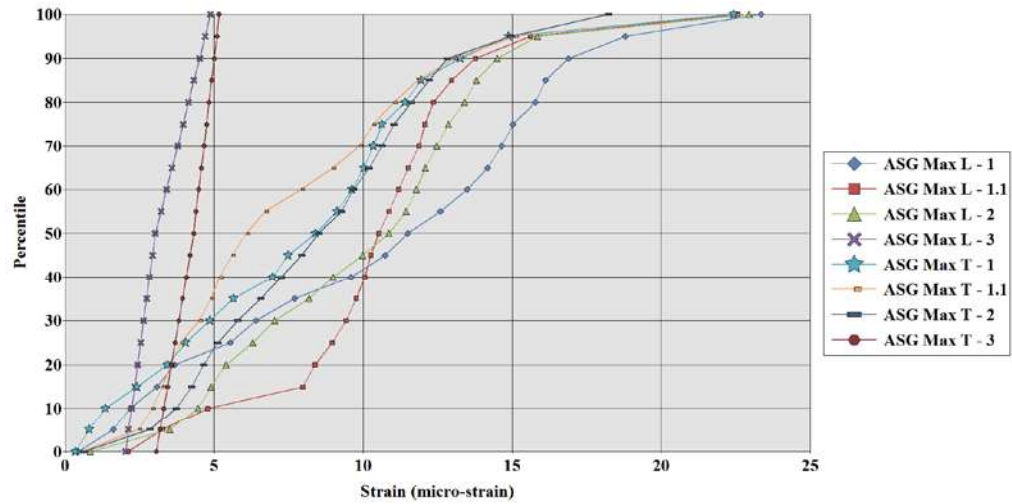


Figure 3.5: Medford Strain Percentiles by Axle Type-Excluding Two Axle Vehicles.

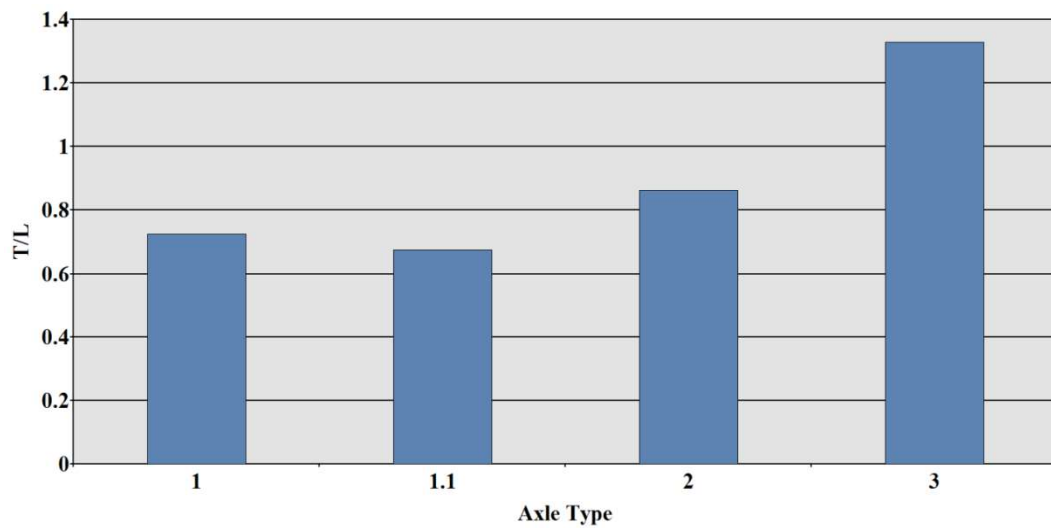


Figure 3.6: Medford Longitudinal and Transverse Strain Comparison.

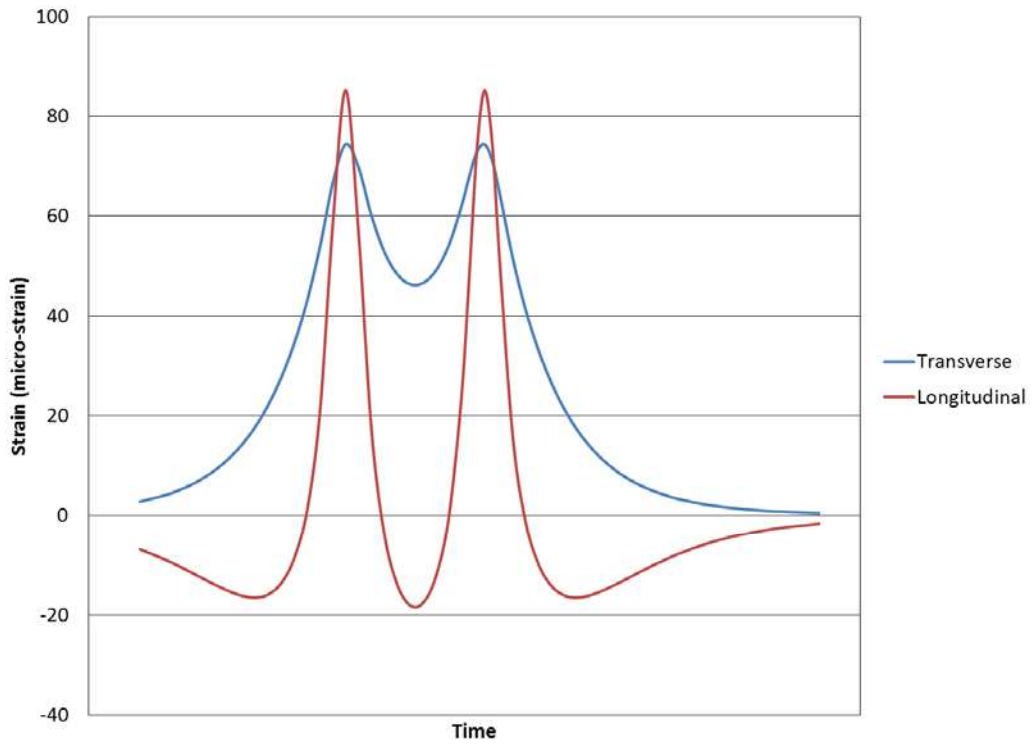


Figure 3.7: Theoretical Strain Response from Tandem Axle.

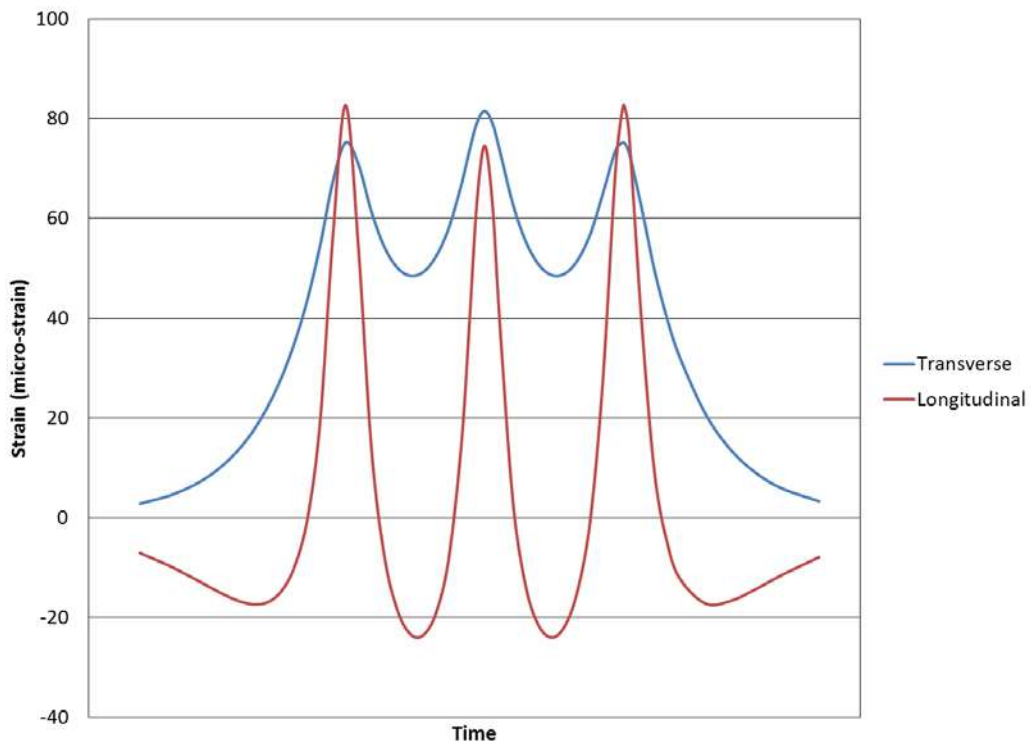


Figure 3.8: Theoretical Strain Response from Tridem Axle.

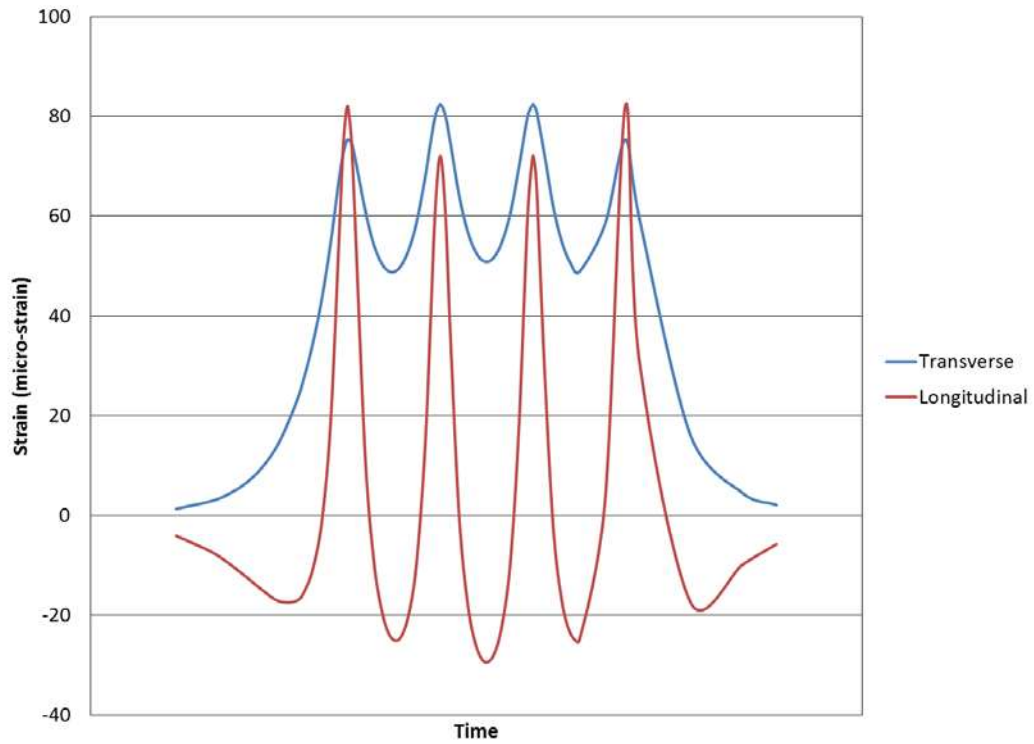


Figure 3.9: Theoretical Strain Response from Quad Axle.

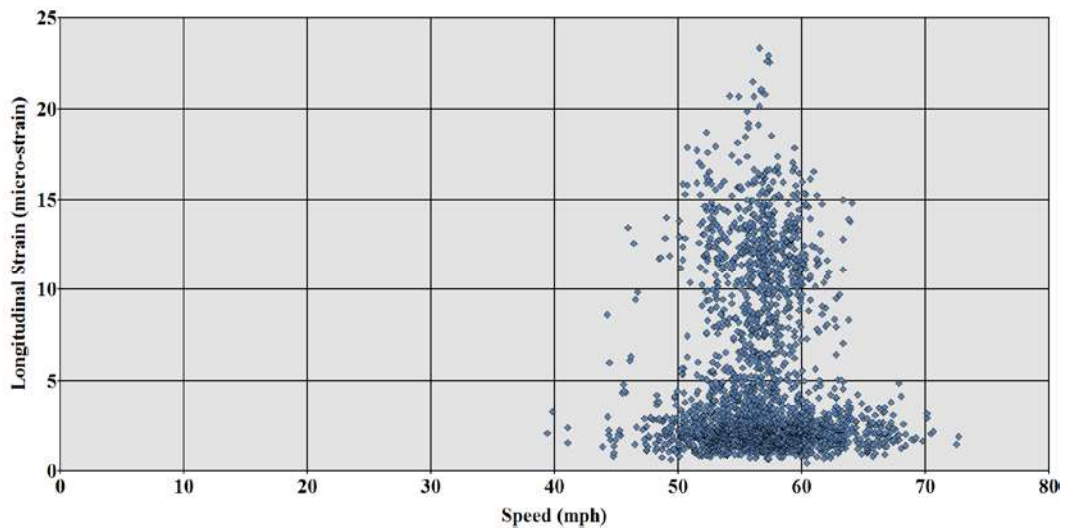


Figure 3.10: Medford Longitudinal Strain and Speed including all Vehicles.

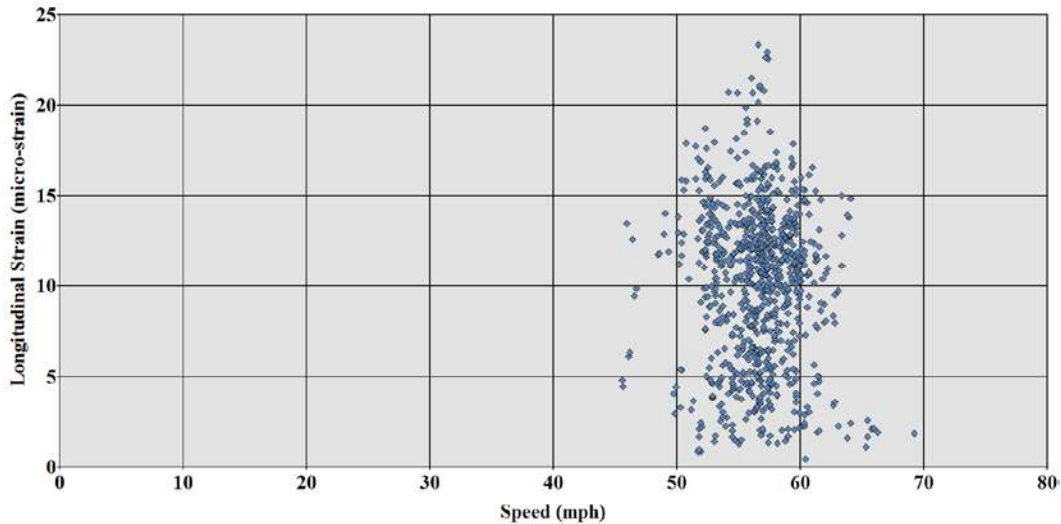


Figure 3.11: Medford Longitudinal Strain and Speed Excluding Two Axle Vehicles.

3.2 REDMOND

3.2.1 Site Description and Scope of Data

The instrumented pavement section on US 97 in Redmond was constructed in June 2008. Instrumentation included axle sensing strips and nine asphalt strain gauges, with the same layout shown previously for the Medford section (Figure 3.1). Data were collected on 11 dates from October 2008 through November 2009. A total of 2,989 files were collected which comprised 2,630 individual vehicle events that were processed. The discrepancy between the number of files that were collected and the number of vehicles events that were able to be processed is mainly due to a large number of files from September 29, 2009 being collected over 0.4 seconds instead of 4 seconds. Other files that were not able to be processed from this site included only electronic noise, low voltage readings on the axle sensing strips, or partial vehicles being captured. From those vehicle events there were a total of 7,884 axles for which the corresponding longitudinal and transverse strain was recorded.

Figure 3.12 shows the distribution of the number of axles per vehicle. The majority of the vehicles collected were two axle vehicles and there 20% five axle vehicles. The axle type distribution is shown in Figure 3.13. Approximately one third of the axle group types were steer, single or tandem axles, respectively. The remainder of the axles were tridem and quad axles.

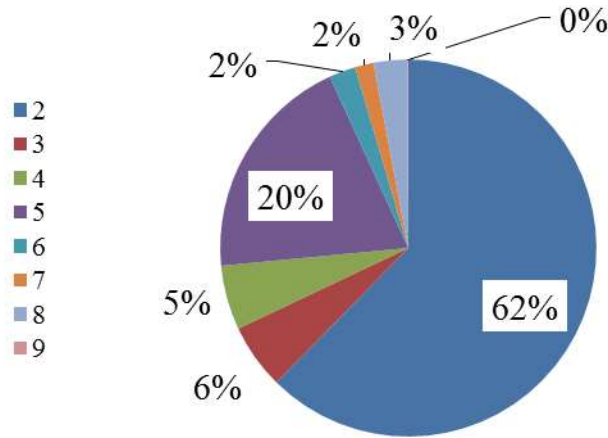


Figure 3.12: Redmond Distribution of Axles per Vehicle.

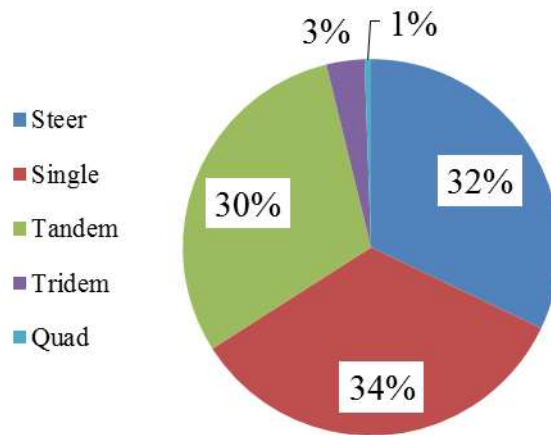


Figure 3.13: Redmond Axle Type Distribution.

3.2.2 Results and Discussion

The percentiles of longitudinal and transverse strain by axle type are presented in Figure 3.14. The legend is the same as used for the Medford plots in which “Max T” and “Max L” represent the maximum strain induced by an axle event measured by the transverse and longitudinal gauges, respectively. As described earlier, “1.1” represents a steer axle and “1”, “2”, “3”, and “4” are single, tandem, tridem and quad axles, respectively. It can be seen that the lowest strain percentiles are in the transverse direction from steer and single axles with the 90th percentile less than 20 $\mu\epsilon$. As done for the Medford site, the percentiles were recalculated without two axle vehicles and are shown in Figure 3.15. The most noticeable change from Figure 3.14 to Figure 3.15 is the increase in strain percentiles from the single and tandem axles as expected from presumably heavier vehicles.

The same trend between longitudinal and transverse strain observed in Medford was apparent in the responses measured at Redmond. Figure 3.16 shows the average of the ratio of the transverse strain divided by the longitudinal strain from each axle event. The tridem axle was the only axle type that did not have a reduction in transverse and longitudinal microstrain. As discussed for the Medford site, linear-elastic analysis showed that the transverse strain is greater than the longitudinal strain for the middle axles of tridem and quad axle sets.

The longitudinal strain versus speed is presented in Figures 3.17 and 3.18 for all vehicles and after removing two axle vehicles, respectively. In both cases, there is no distinguishable trend between strain and speed which again means the strain variation is not influenced primarily by vehicle speed.

The 10th, 50th and 90th percentile longitudinal strain values for tandem axles on each date are presented in Figure 3.19. It can be seen that there is a seasonal trend in the strain responses due to the temperature sensitivity of the asphalt concrete. The lowest strain responses were observed during the winter months and the highest strain response was recorded in August. It is also noteworthy that there is no reduction in strain values over time as evident by similar strain responses taken in November 2008 and in November 2009. This observation indicates that there was no damage to the pavement structure over that time period.

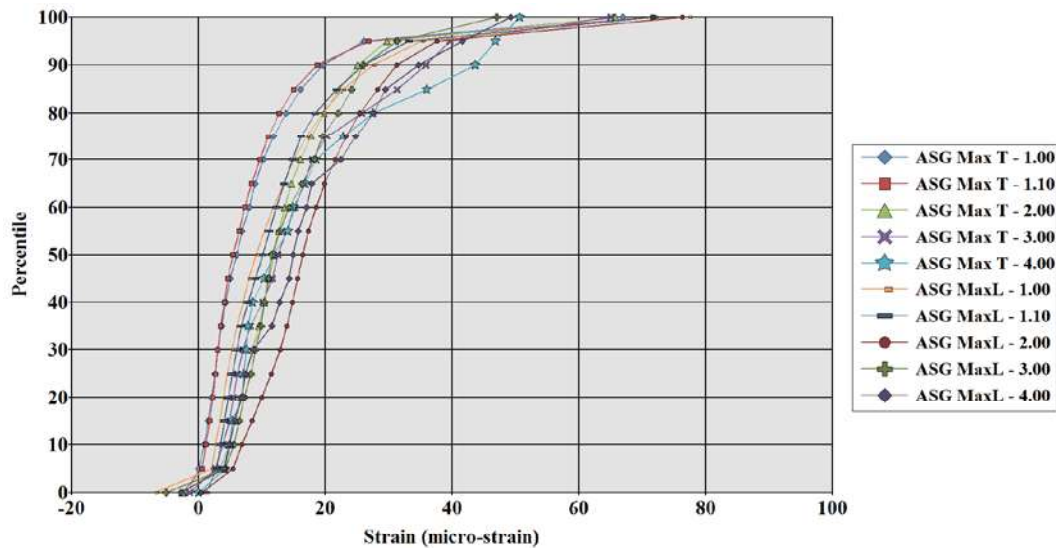


Figure 3.14: Redmond Strain Percentiles by Axle Type.

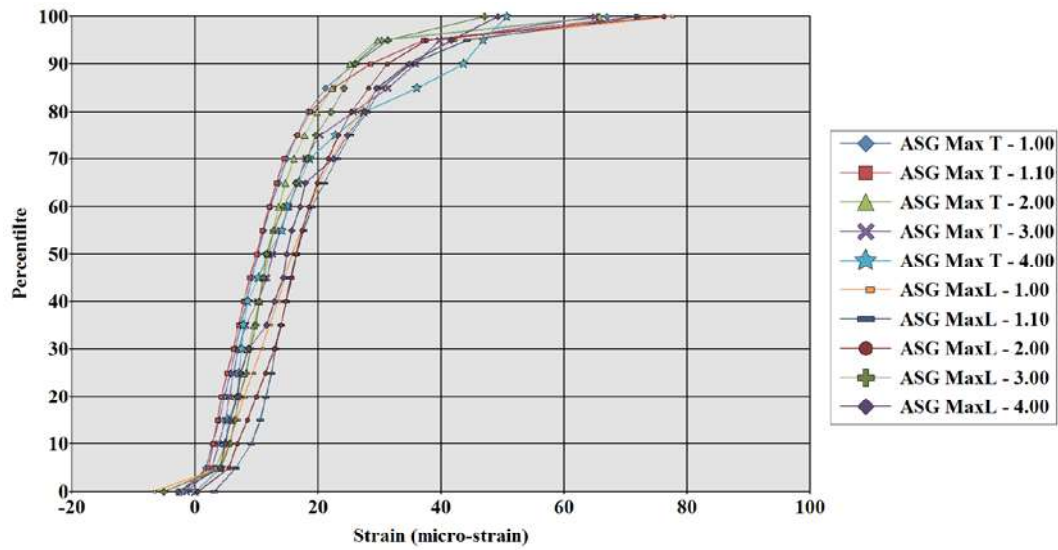


Figure 3.15: Redmond Strain Percentiles by Axle Type Excluding Two Axle Vehicles.

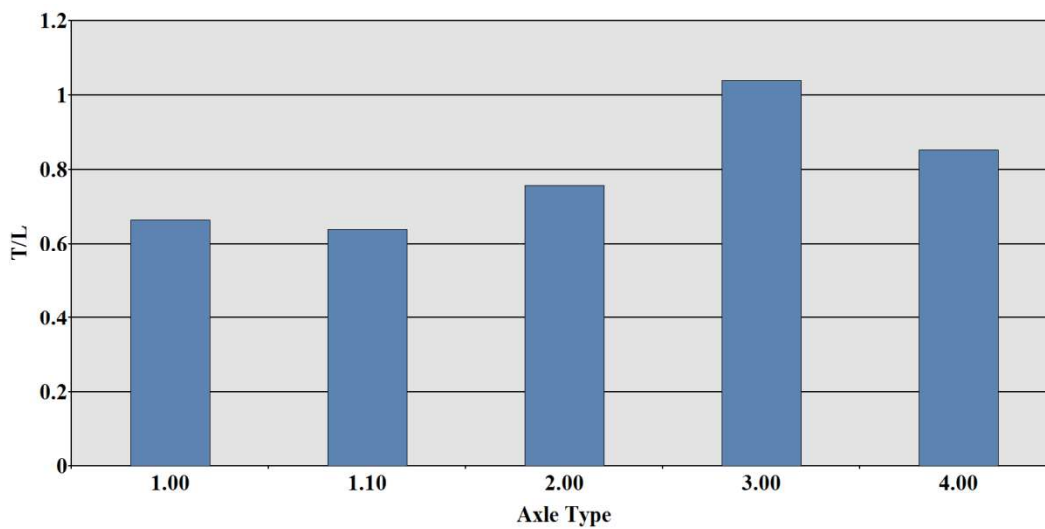


Figure 3.16: Redmond Longitudinal and Transverse Strain Comparison.

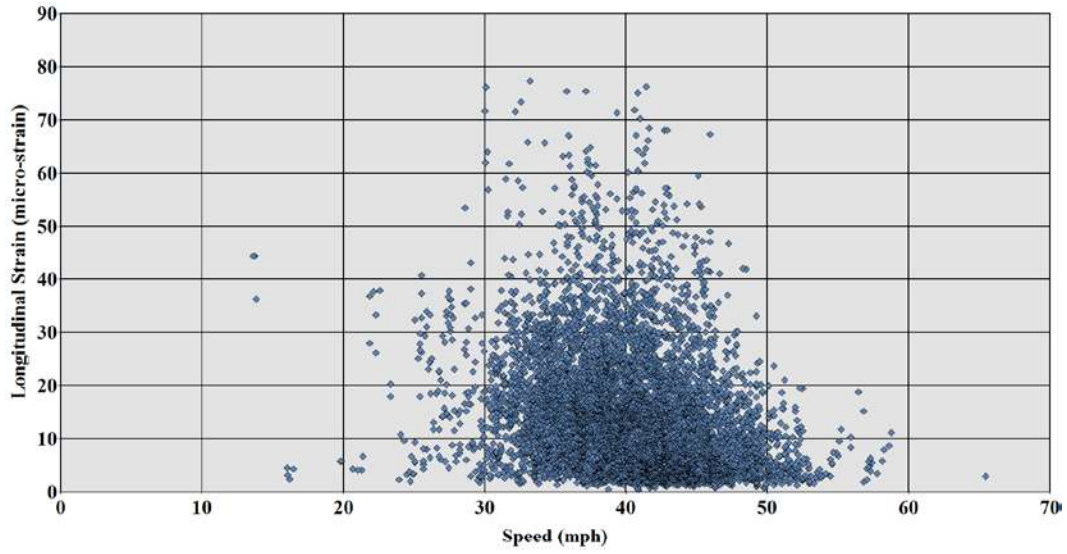


Figure 3.17: Redmond Longitudinal Strain and Speed including all Vehicles.

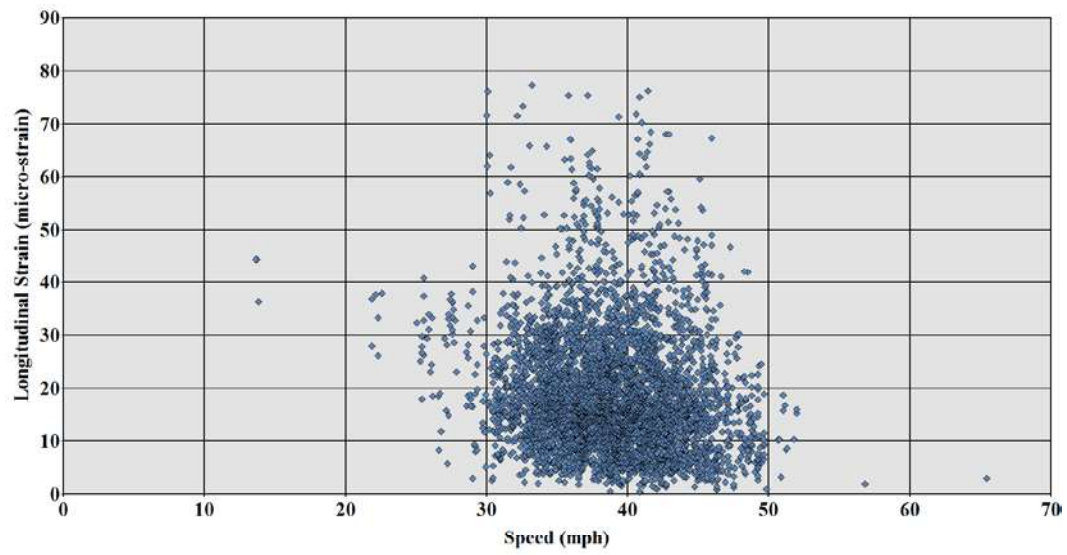


Figure 3.18: Redmond Longitudinal Strain and Speed Excluding Two Axle Vehicles.

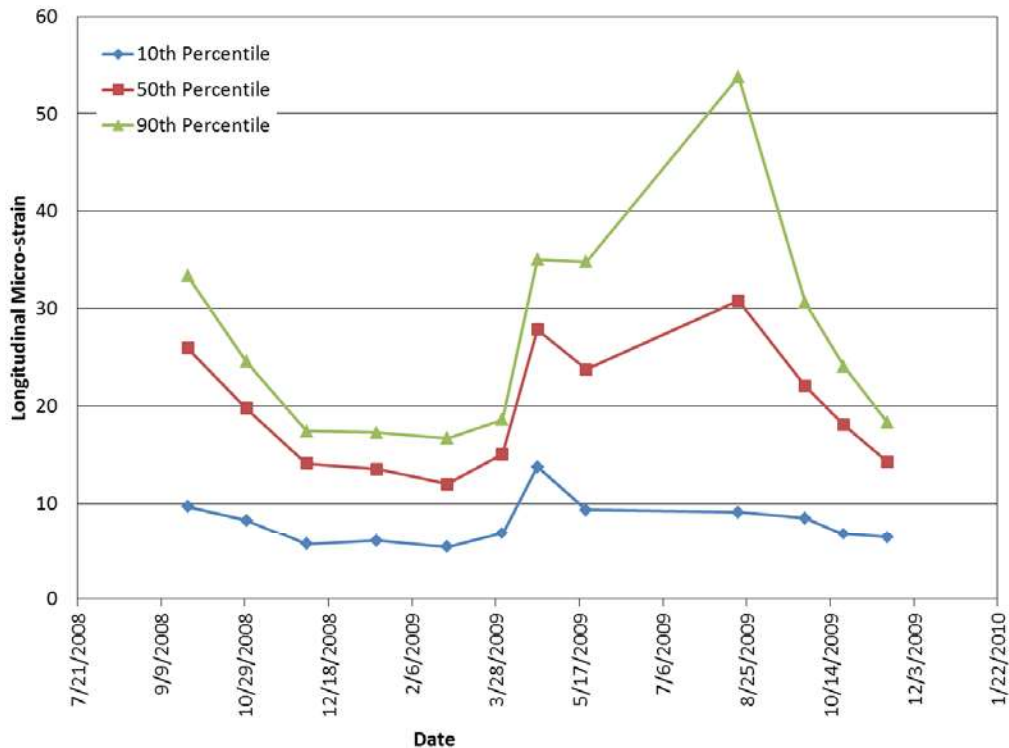


Figure 3.19: Redmond Longitudinal Strain by Date

3.3 DEVER-CONNER

3.3.1 Site Description and Scope of Data

The Dever-Conner instrumented pavement sections on I-5 were constructed during the summer of 2007. Data were collected on twelve dates between October 2008 and November 2009. The Dever-Conner site had two strain gauge arrays of 12 gauges each with six gauges oriented in the longitudinal direction and six in the transverse direction, as shown in Figure 3.20. The first strain gauge array was placed over an aggregate base and the following gauge array was placed over a rubblized Portland cement concrete base. Axle sensing strips were placed between the strain gauge arrays. It should be noted that there were five dates in which there was no data collected from the gauge array over the rubblized concrete base.

A total of 3,605 files were collected and 3,380 individual vehicle events were processed. Some of the files collected were not able to be processed due to electronic noise, low voltage responses on the axle sensing strips, and partial vehicles being captured. Data collected at the Dever-Conner site included a significantly higher percentage of vehicles with more than two axles, as shown in Figure 3.21. The majority of the vehicle events (56%) were five axle vehicles and only 16% were from two axle vehicles. Figure 3.22 shows that the increase in vehicles with more than two axles is also apparent in the axle type classification. The majority of axles were classified as tandem; steer and single axles represented 21 and 19% of the total axle types, respectively.

Although there were 495 and 352 axles classified as tridem and quad, these events only accounted for 3 and 2% of the total axle events, respectively.

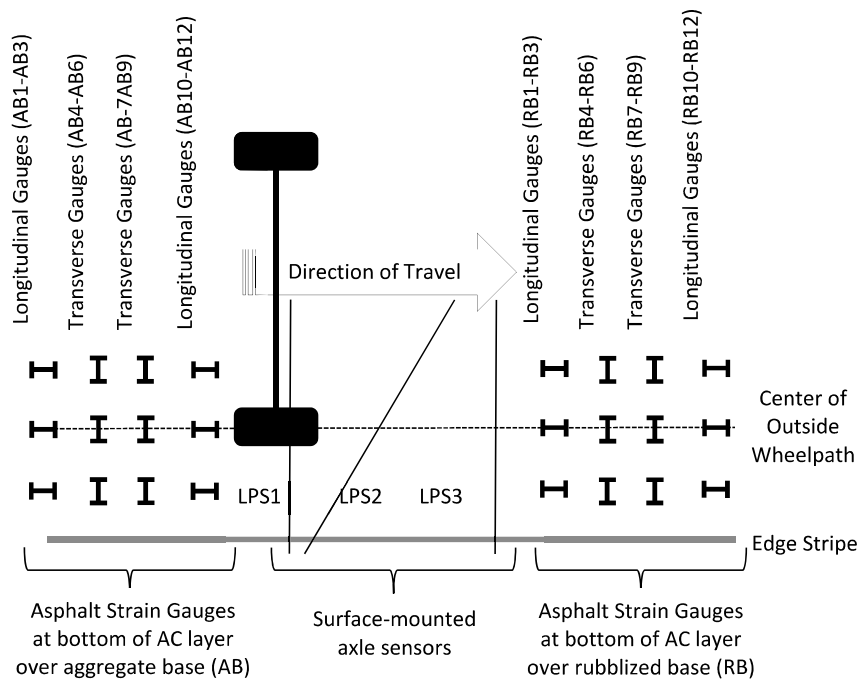


Figure 3.20: Dever-Conner Instrumentation Layout.

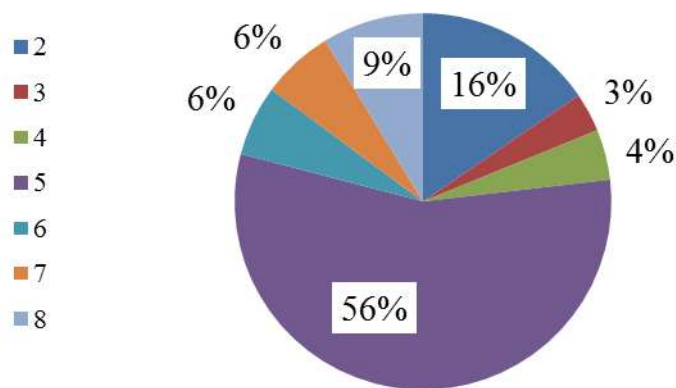


Figure 3.21: Dever-Conner Distribution of Axles per Vehicle.

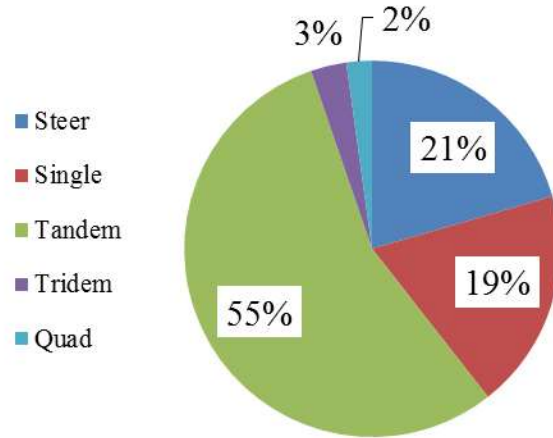


Figure 3.22: Dever-Conner Axle Type Distribution.

3.3.2 Results and Discussion

The strain percentiles for the aggregate and rubblized base layers are presented in Figures 3.23 and 3.24, respectively. The legend is the same as used previously in the percentile plots for the Redmond and Medford sites. In Figure 3.23, the highest strain percentiles are in the longitudinal direction for steer, single, and tandem with the 90th percentile strain just under 20 $\mu\epsilon$. The strain percentiles in Figure 3.24 for the rubblized base section are smaller with the 90th percentile strain around 5 $\mu\epsilon$ for all gauge orientations and axle types. In the rubblized base responses, there is no distinguishable separation between percentiles for gauge orientation or axle type.

Figure 3.25 shows a comparison of longitudinal and transverse gauges for both base types. For the aggregate base, the ratios of transverse over longitudinal strain are similar to those observed in the Medford and Redmond sites with values 0.70, 0.60, and 0.82 for steer, single, and tandem axles, respectively. The rubblized base did not show this trend and all ratios were greater than one, indicating that the measured transverse strain was greater than the measured longitudinal strain. Although this trend for the rubblized base section was unexpected, it is likely due to the very low strain responses measured and is exacerbated on tridem and quad axles by the phenomenon of higher transverse strains from the middle axles, presented previously in Figures 3.6, 3.7, and 3.8. A previous NCAT Test Track investigation (*Willis and Timm 2009*) found that strain gauge repeatability was within 12 $\mu\epsilon$. Thus, it could be that the extremely low strain values from the rubblized section are within the measurement precision of the gauge itself.

It can be seen in Figure 3.26 that there is no distinguishable trend between the speed of the vehicle and the longitudinal strain. Two axle vehicles were included in this plot (excluded in some of the Redmond and Medford plots) because they only comprised 15% of the total vehicles processed and therefore do not overshadow the other vehicles.

Figure 3.27 shows the 90th percentile longitudinal and transverse strain values for the aggregate and rubblized base. The seasonal trend of strain over the annual temperature cycle can be seen in Figure 3.27 with higher strains occurring in the summer months when the asphalt concrete

modulus is reduced. The trend is apparent for both base types even with less dates available and lower magnitudes in the rubblized base. Again, it must be noted that data were not collected from the rubblized base gauges on the first five collection dates.

A direct comparison of the strain measured over the aggregate base and rubblized base is summarized in Figure 3.28. For each axle event, a paired comparison was made in which the greatest strain measured over the aggregate base was compared to the corresponding greatest strain measured over the rubblized base. The ratio of strain over the rubblized base divided by strain over the aggregate base was calculated for each axle event and the average for each axle type is presented in Figure 3.28. It can be seen that for all orientations and axle types that the strain over the rubblized base was less than 50% of the strain over the aggregate base. The transverse strain ratios were higher than the longitudinal strain ratios for all axle types. The rubblized base significantly reduced the strain induced at the bottom of the asphalt contact which improves the pavements resistant to traditional, bottom-up fatigue cracking.

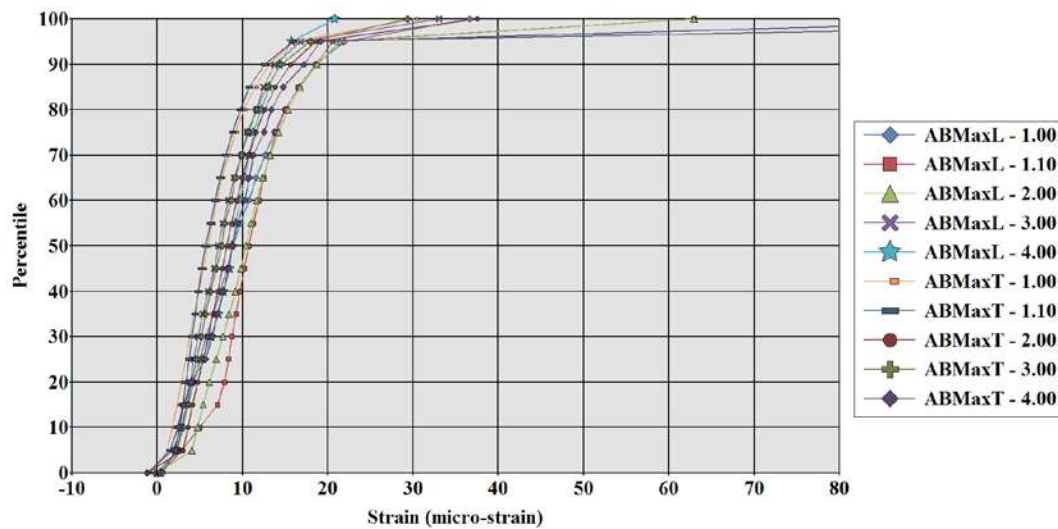


Figure 3.23: Dever-Conner Strain Percentiles by Axle Type over Aggregate Base.

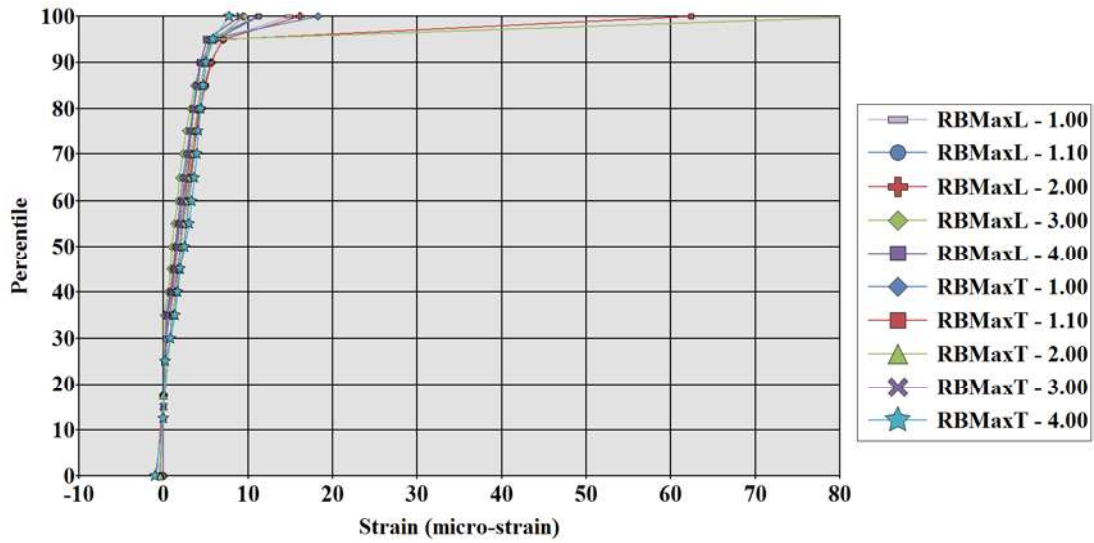


Figure 3.24: Dever-Conner Strain Percentiles by Axle Type over Rubblized Base.

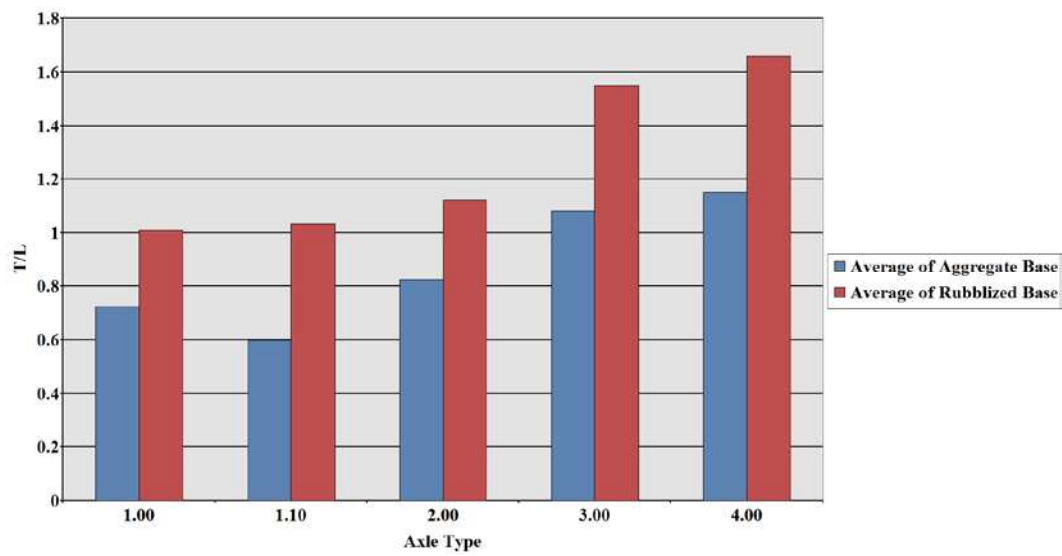


Figure 3.25: Dever-Conner Longitudinal and Transverse Strain Comparison.

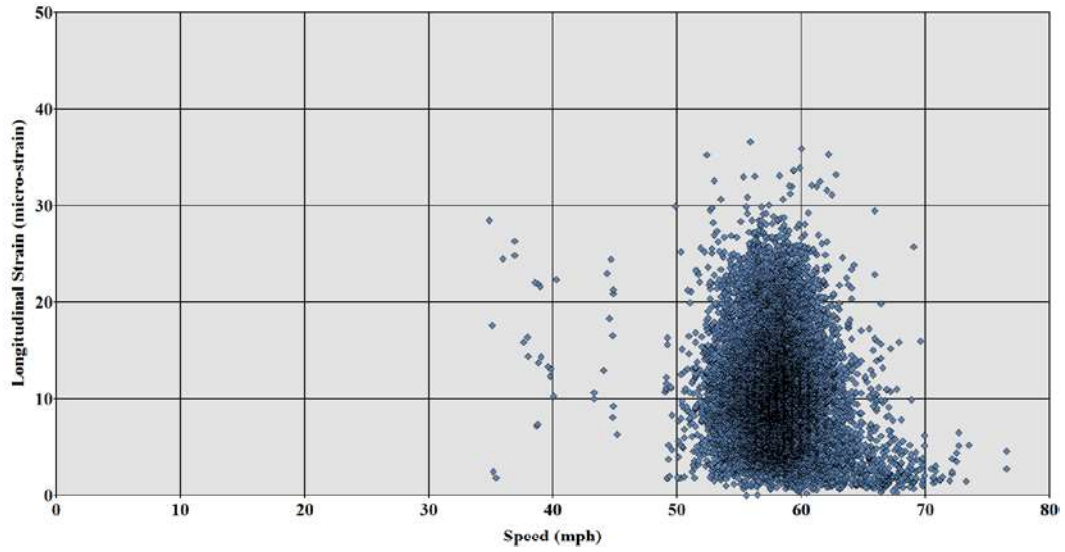


Figure 3.26: Dever-Conner Longitudinal Strain and Speed including all Vehicles

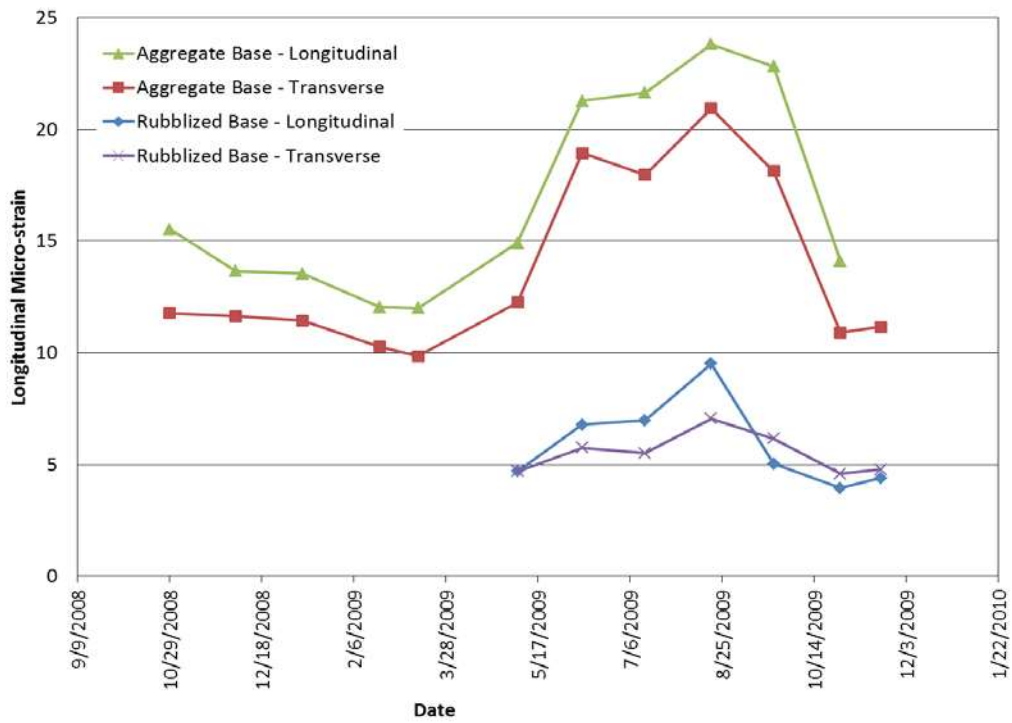


Figure 3.27: Dever-Conner 90th Percentile Strain from Five Axle Vehicles over Time

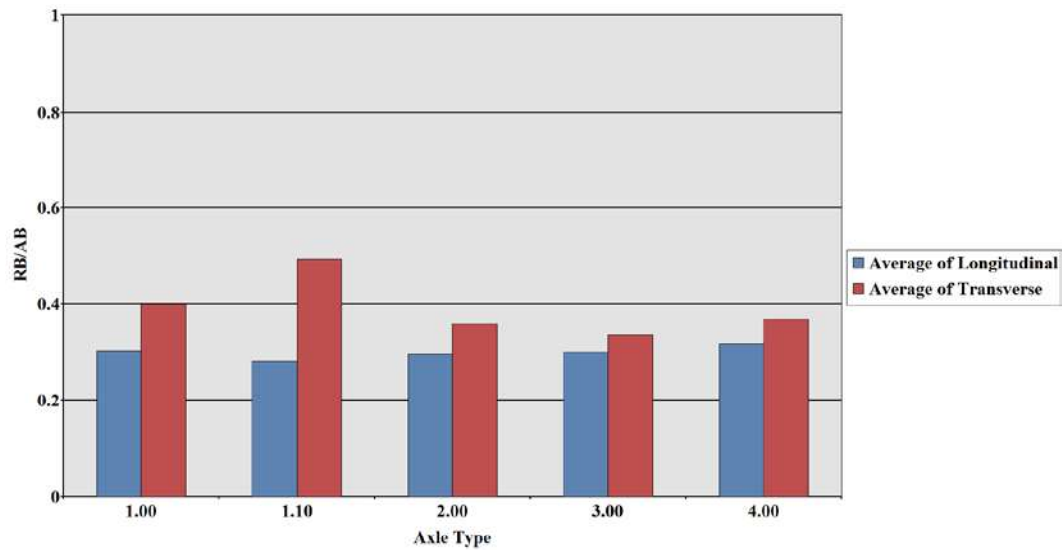


Figure 3.28: Dever-Conner Strain Comparison from Aggregate to Rubblized Base

3.4 COMPARISON BETWEEN TEST SITES

The strain induced on a pavement by a passing vehicle is a function of vehicle weight, environmental conditions, and the pavement layers. Therefore, direct comparison between sites is difficult. To mitigate the impact of environmental conditions, testing dates in November 2009 were chosen for further comparison (Medford was only collected in November 2009). The average strain value from each site recorded in November 2009 is presented in Figure 3.29. The error bars show the standard deviation. Similar strain values were recorded at Redmond and Dever-Conner Aggregate Base. The Dever-Conner Rubblized Base was significantly lower than all other sites. This highlights the effect of the rubblized base at reducing strain levels. The Medford, Redmond, and Dever-Conner Aggregate Base sites had similar cross sections, as shown in Figure 3.30. It was expected that the similar cross sections would result in similar strain responses. However, the Medford strains were slightly lower which was likely due to the large amount of two axle vehicles presented in Figure 3.2.

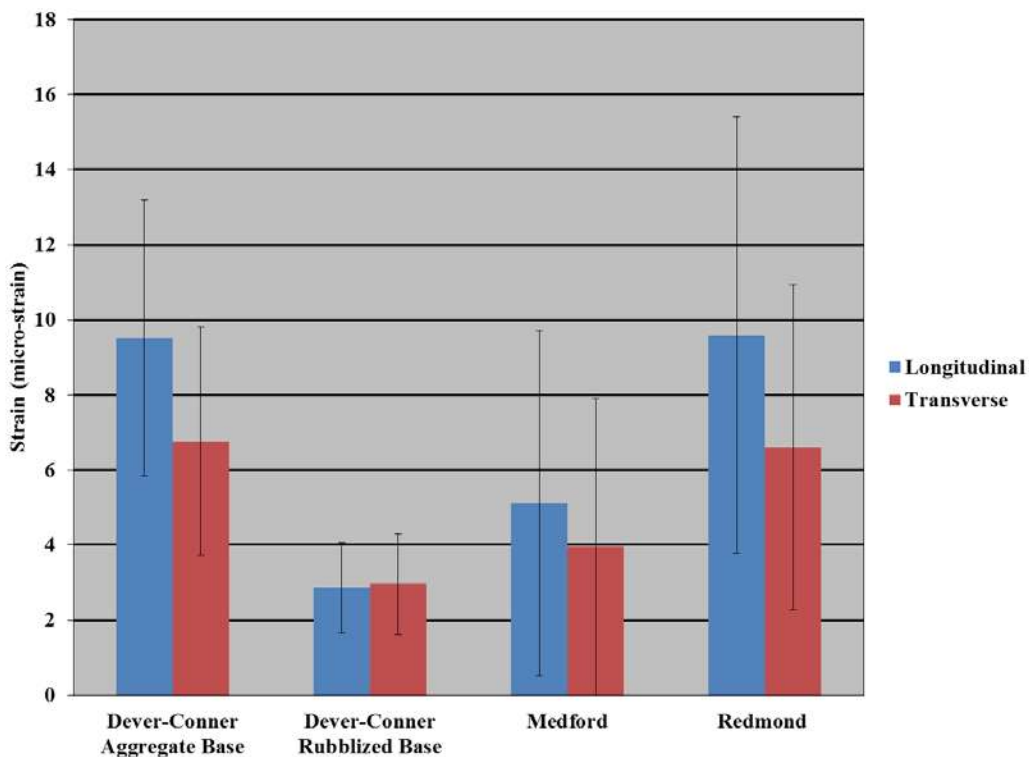


Figure 3.29: Comparison of Average Strain Recorded in November 2009

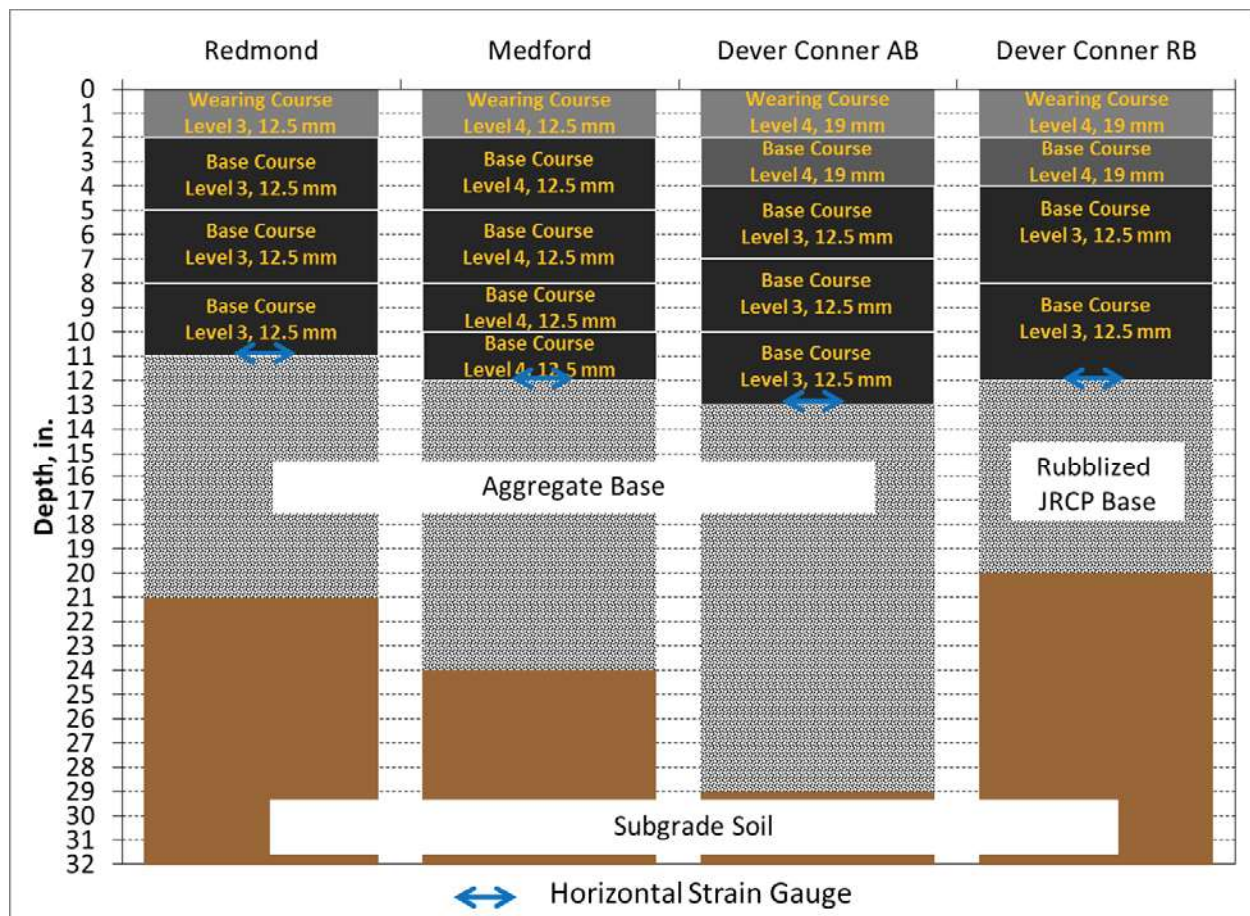


Figure 3.30: Pavement Cross Sections.

4.0 TECHNOLOGY TRANSFER

The last objective of Phase II was to provide user's guides on working with the DADiSP templates and Access databases that will enable future analyses as needed by ODOT. These guides have been developed as stand-alone appendices. Appendices A, B and C contain detailed instructions for using the DADiSP templates for each test site while Appendices D, E and F contain guidance on using the Access databases. Note the large number of sub-appendices correspond to the many file formats encountered in the raw data archives.

5.0 SUMMARY

The objectives of Phase II of this project included documenting the data processing schemes and database development from each site, characterizing the in situ pavement responses from each site, comparing the pavement responses between the sites and providing user's guides for using the processing templates. Based on the work presented herein, the following conclusions and recommendations are made:

- Most of the collected data could be processed from each test site and assembled into site-specific databases. Instances where the data could not be processed usually resulted from erroneous data files and improper sampling durations.
- Analysis of the data followed expected trends where the transverse strain was generally lower than longitudinal strain. The exceptions, based on axle type, were demonstrated to follow layered elastic theory.
- Seasonal trends were clearly evident in the data sets that had multiple dates. These trends may be used for future M-E analysis and simulation of the sections.
- The rubblized base layer had a significant impact on measured strain values at the Dever-Conner site. Paired measurements showed over a 50% reduction in strain response.
- Further analysis of the data may be accomplished using the assembled databases and user's guides provided in the appendix of this report.

6.0 REFERENCES

Scholz, T.V. *Instrumentation for Mechanistic Design Implementation*. Final Report. OTREC-RR-10-02. Oregon Transportation Research and Education Consortium (OTREC), 2010.

Timm, D.H., and M.C. Vrtis. *Mechanistic Design Data from ODOT Instrumented Pavement Sites-Phase I Report*. Draft Report. National Center for Asphalt Technology, Auburn University, 2015.

Timm, D.H., and A.L. Priest. *Flexible Pavement Fatigue Cracking and Measured Strain Response at the NCAT Test Track*. Proceedings of the 87th Annual Transportation Research Board, Washington, D.C., 2008.

Willis, J.R., and D.H. Timm. *Repeatability of Asphalt Strain Gauges*. NCAT Report 09-07, National Center for Asphalt Technology, Auburn University, 2009.